CHAPTER 3

SYNTHESIS AND CHARACTERIZATION TECHNIQUES

The samples were prepared by conventional solid state reaction method and characterized by X-Ray diffraction (XRD) studies of the phases present, Micro structural Analysis using Scanning Electron Microscope (SEM), measurement of dielectric properties in rf range upto 1 MHz as well as in microwave range in X-band (8 – 12 GHz), tracing of P-E Hysteresis Loop and Impedance Spectroscopy. These are briefly described below.

3.1 Synthesis of ceramics and sample preparation

Ceramics can be prepared by solid state reaction methods or wet chemical methods [West (2014); Moulson et al. (2003)]. Due to being simple, easy and straight forward, the solid state reaction method is still widely used for preparing bulk amount of ceramics. In this method, reaction proceeds in solid state for which, it is essential to bring particles of reactants into contact and raise the temperature. This is facilitated by increasing the surface area of the reactants and speeding up the reaction. This is achieved by fine grinding, mixing and heating. The grinding can be done manually by using mortar-pestle. Agate mortars and pestles are useful since they are non-porous, readily cleaned and do not contaminate samples. For labour saving, grinding is done in ball mills where the starting compounds are placed in a container having small balls. This container is rotated. The balls have tumbling motion inside and crush the particles from various directions giving rise to fine powder. In planetary ball mills, the container is rotated at very high speed. To facilitate mixing, by whatever method, a liquid such as

water or an organic liquid (usually acetone) is often added and then removed by drying at the end of the mixing stage.

Certain materials can be prepared by using the so called combustion synthesis where starting materials are chosen that react together exothermically. Once a reaction is initiated, sufficient heat is generated so that for high temperatures are attained and reaction completes rapidly. Materials can also be prepared by using high energy ball milling without providing external heat. High temperatures may be generated locally as the mechanical energy is transformed into heat which speeds up inter-particle diffusion and the product phase is formed. Products with high chemical homogeneity are obtained by resorting to wet chemical methods such as sol-gel method. In this a homogeneous solution containing all the cationic ingredients in the desired ratio is first prepared. The solution is gradually dried so that it transforms into a viscous *sol* containing particles of colloidal dimensions and then to a homogeneous solid known as a *gel*. The gel is then fired at high temperatures to crystallise the final product. In these alternative methods, often the reagents are costly and difficult to handle on a large scale and considerable research may be required to optimise the synthesis of a particular material. For these reasons, conventional solid state reaction method is usually used as it is quick, easy and versatile. Hence in the present study conventional solid state synthesis route has been followed.

The samples were prepared by conventional solid state reaction method. This involves weighing the starting compounds in appropriate amounts, mixing, high temperature firing/calcinations, intermediate grinding followed by sintering. The details of the starting materials are given in Table 3.1. High purity powders were mixed by ball milling and then calcined at appropriate temperatures and duration. Then small amounts of 2% Polyvinyl Alcohol (PVA) solution was added to the calcined powders and

thoroughly mixed in a mortar pestle. The powders were then pelletized with the help of hydraulic press by using 15 mm cylindrical die-cast and 2.3cm x 1cm rectangular die-cast. The pressure applied varied from 60 KN to 80KN. The pellets were then sintered. The details of preparation of electronic ceramic $Ba_{1-x}Sr_xTiO_3$, $BaFe_xTi_{1-x}O_3$ and $BaTi_{1-x}Sn_xO_3$ samples are given in Chapters 5, Chapter 6 and Chapter 7 respectively where they are described in detail.

Table 3.1: Details of the starting materials used for preparation of $Ba_{1-x}Sr_xTiO_3$, $BaFe_xTi_{1-x}O_3$ and $BaTi_{1-x}Sn_xO_3$ samples

Material	**Grade**	**Minimum Assay(%)**	**Manufacturer**
$BaCO_3$	Analytical	99.5	Merck
Fe_2O_3	Analytical	99.5	Merck
TiO_2	Analytical	99.5	Merck
$SrCO_3$	Analytical	99.5	Merck
SnO_2	Analytical	99.5	Merck

A flow chart of the whole process including characterization is shown in Figure 3.1.

3.2 Characterization Techniques

The ceramic samples were characterized by using X-Ray Diffraction (XRD) and Scanninig Electron Microscopy (SEM). Dielectric permittivity, loss and impedance measurements at frequencies below 1 MHz were carried out by using Novocontrol Alpha – A analyser. Dielectric measurements at microwave frequencies were made by using Keysight E5071C Network Analyzer. P-E hysteresis loops were recorded by using AixACCT systems Analyzer 2000E, Germany. These are briefly described below.

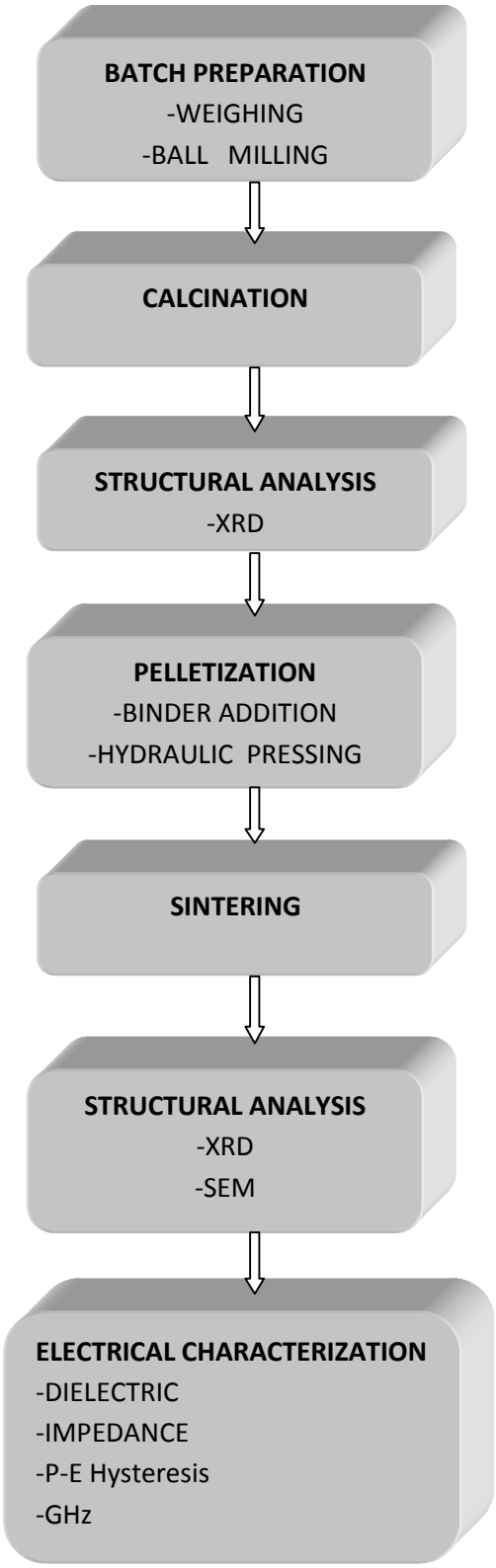

Figure 3.1: A schematic flow chart of sample preparation and characterization

3.2.1 X-Ray Diffraction (XRD)

X-ray diffraction (XRD) is a versatile, non-destructive technique that reveals detailed information about crystallographic structure of natural and manufactured materials. It is routinely used for phase identification and determination of unit cell dimensions. Crystalline substances behave as three dimensional diffraction gratings for X-rays having wavelengths similar to the spacings of planes in a crystal lattice. X-rays, when fall on crystals undergo diffraction. When the X-ray wave length (λ) and plane spacings (d) satisfy the Bragg condition $2d \sin\theta = n\lambda$ constructive interference in the diffracted rays occur and a peak in the intensity in observed. A recording of this intensity as function of 2θ is what is called X-ray diffraction pattern (2θ is the angle between diffracted and undiffracted beam) and contains number of sharp intensity peaks for crystalline materials. This pattern is analysed and information about spacing 'd' and related crystal structure is obtained [West (2014); Cullity (1956)].

X-rays are electromagnetic radiation of wavelength $\sim$1 A^0 (10^{-10} m) and are produced when high-energy charged particles, e.g. electrons accelerated through high voltages, collide with some target matter. Some general target materials are Cr, Fe, Cu, Mo, Ag out of which Cu is commonly used. X-rays are generated by a cathode ray tube having a filament that emits electrons when heated. These electrons are accelerated by several kV (~ 30 kV) towards an anode . The electrons strike the target, usually a piece of copper, attached to the anode. The incident electrons have sufficient energy to ionise some of the Cu 1*s* (*K* shell) electrons. An electron in an outer orbital (2*p* or 3*p*) immediately drops down to occupy the vacant 1*s* level and the energy released in the transition appears as X-radiation. The radiation corresponding to the $2p \rightarrow 1s$ transition

is called $K\alpha$, and has has a wavelength of 1.5418 A . The 3 $p \rightarrow 1s$ transition, called $K_{\beta,}$ has wave length of 1.3922 A˚. The $K\alpha$, transition occurs much more frequently than the $K\beta$, and is used in diffraction experiments. Also the $K\alpha$ radiation is a doublet, denoted as $K\alpha_1$ having wavelength of 1.54051 A˚ and $K\alpha_2$ of 1.54433 A. The 2p electron has total angular momentum number $j = l \pm s$, where l denotes the orbital quantum number and s denotes the spin quantum number so that j = 3/2 or 1/2 as l =1for a 2p electron. The two possible transitions are then 2 p $_{1/2} \rightarrow$ 1 $s_{1/2}$ (denoted as $K\alpha$) and 2 p $_{3/2} \rightarrow$1 s $_{1/2}$ (denoted as $K\alpha_2$). A monochromatic X – ray beam (Cu $K\alpha_1$) produced by adequate filtering of the background and characteristic radiations is focussed and directed towards the sample. For Cu radiation, a sheet of Ni foil is a very effective filter. The energy required to ionise 1s electrons of Ni corresponds to a wavelength of 1.488 A, which lies between the values for the $K\alpha$ and $K\beta$ lines of the Cu emission spectrum. Cu $K\beta$ radiation, therefore, has sufficient energy to ionise 1s electrons of Ni whereas Cu $K\alpha$ radiation does not. Ni foil is effective in absorbing the Cu $K\beta$ radiation and most of the white radiation, leaving a monochromatic, reasonably clean beam of $K\alpha$ radiation.

When the incident beam strikes a powder sample, diffraction occurs in every possible orientation of 2θ .The diffracted beam may be detected by using a movable detector such as a Geiger counter, which is connected to a chart recorder. In normal use, the counter is set to scan over a range of 2θ values at a constant angular velocity. Routinely, a 2θ range of 5 to 90 degrees is sufficient to cover the most useful part of the powder pattern. The scanning speed of the counter is usually 2θ of 2 degrees min^{-1} and therefore, about 30 minutes are needed to obtain a trace (diffraction pattern). Based on the principle of X-ray diffraction, a wealth of structural, physical and chemical information about the material investigated can be obtained.

The most important use of the powder method is in the identification of crystalline phases or compounds. Each crystalline phase has a characteristic powder XRD pattern which can be used as a fingerprint for identification purposes. The main factors determining the XRD patterns are (i) size and shape of the unit cell and (ii) the atomic number and position of atoms in the unit cell. Change in peak positions indicates change in *d*-spacings i.e. change in unit cell dimensions. For the same structure but with different types of atoms present in the cell, intensities of the peaks would differ. This is because atoms with different atomic numbers have different scattering powers.

An extremely useful reference source for using XRD patterns for identification of unknown crystalline materials is the *Powder Diffraction File* (International Centre for Diffraction Data, USA). It was earlier known as the ASTM or JCPDS file. This contains the XRD patterns of more than 300 000 materials and around 2000 new entries are added per year. In the search indices, materials are classified according to either their most intense peaks or the first eight lines in the XRD pattern in order of decreasing *d*-spacing. Computer softwares make it possible to finish identification of an unknown usually within a few minutes of obtaining its XRD pattern [West (2014)].

For the analysis of a powder pattern for identification purposes normally most attention is paid to to the *d*-spacings but, at the same time, it is also kept in mind that the intensities are roughly correct. Once the structure has been identified, it is confirmed and unit cell dimensions are determined by using the Rietveld refinement method. It is an extremely valuable method for materials in which the approximate structure type may be known but for which details need to be determined, or confirmed. Rietveld refinement is a whole pattern refinement. In this procedure, the experimental powder XRD profile is compared with a calculated profile, whose parameters are adjusted by refinement. A starting model for a crystal structure is chosen from the

analysis of the experimental pattern and a powder XRD profile is calculated. The Rietveld refinement is essentially a least squares procedure where the approximate structural data obtained from the analysis of the XRD pattern is taken as an initial guess. The parameters are refined iteratively so that experimental and calculated patterns match. The method was developed initially for processing powder neutron diffraction data. It has since been extended to XRD also [West (2014)].

To check the phase formation in the samples reported in the thesis, powder X-ray diffraction was done at different stages of synthesis (i.e. after calcination and after sintering). The calcined powder and powder of sintered pellets were ground and powder X-ray diffraction patterns were recorded using an X-ray Diffractometer (Rigaku MiniflexII , Desktop X-Ray D) employing Cu-Kα radiation with Ni filter. Rietveld refinement procedures were carried out for obtaining the refined values of unit cell parameters by using Fullprof software [Fullprof (2016)].

3.2.2 Scanning Electron Microscopy (SEM) and Energy Dispersive Spectroscopy (EDS)

Electron microscopy utilizes beam of high energy electron for obtaining an image of an object. It is a versatile tool for providing morphological, structural and compositional information over a wide range of magnification. The resolving power of an optical or electron microscope is given as $n \sin\theta / 0.61 \lambda$ where $n \sin\theta$ is the numerical aperture of the lens and is a function of its light collecting capability. An electron (charge e and mass m) accelerated through a voltage V gains kinetic energy given by $\frac{1}{2} m v^2 = eV$. By using de Broglie relation $\lambda = h / mv$, h being Planck's constant, we get the wave length λ as $h/ \sqrt{(2meV)}$ or $12.3/\sqrt{V}$ A^0. Thus an electron microscope has much larger resoling power than an optical microscope.

Electrons emitted by an electron gun are accelerated and focussed by using electric and magnetic fields produced in the so called electromagnetic lenses. These condenser lenses control the size and angular spread of the incident electron beam. This beam is made to strike the sample where reflection/transmission may occur. Electron microscopes operate in either transmission or reflection. For transmission thin samples (thickness~0.2μm) are used because electrons interact with the material and get absorbed in thicker samples. For situations where it is difficult to make thin samples, high voltage microscopes (~ 1 MV) or finely crushed powder may be used. In reflection mode, sample thickness is not a problem. However, the sample is to be coated with a thin layer of metal (gold), to prevent the build-up of charge on the surface. When the electron beam strikes the sample, the electrons in the beam can interact with the solid elastically or inelastically. In elastic collisions, the energy of electrons remains almost unaltered and the electron beam remains coherent with the incident electron beam. These coherently scattered electrons interfere and produce patterns that can be recorded as in XRD. In inelastic collision the energy of the incident electrons is absorbed by the sample due to which several things may happen: (i) photons (visible or X-rays) may come out (ii) secondary electrons may be emitted (iii) lattice vibrations may get excited resulting in heating of the sample (iv) structural changes known as radiation damage may occur. By utilizing the emitted electrons or radiations, number of imaging, diffraction, analytical and spectroscopic techniques, such as electron probe microanalysis (EPMA) and energy-dispersive analysis of X-rays (EDS, EDX or EDAX) have been developed which are summarized in Figure 3.2. In EPMA and EDX the characteristic X-rays emitted by the elements present in the sample are used. The emission spectra is recorded by scanning their wavelength (wavelength dispersive, WD)

or their energy (energy dispersive, ED). Thus the elements present in the sample are identified and quantitative elemental analysis may be made.

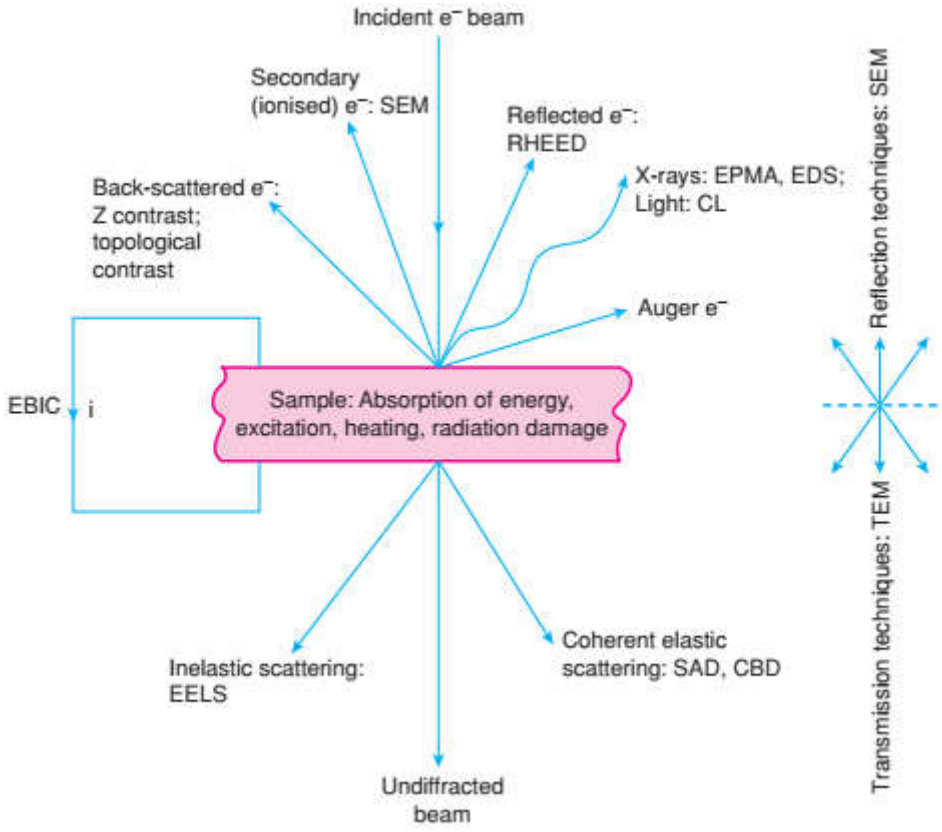

Figure 3.2: Schematic representation of Reflection and transmission signals in SEM and TEM modes [West (2014)].

In SEM, an electron beam is produced by accelerating the electrons from the electron gun through 5–50 keV. This beam, focused to a small spot ~ 50–500 A˚ in diameter on the sample, scans the sample surface. The penetration depth of the electron beam is typically up to 1 μm. The lower limit of resolution with SEM instruments is ~100 Å. Images may be recorded using both secondary electrons and back-scattered electrons, with instrumental conditions optimised for good topographic contrast. The basic principle is shown schematically in Figure 3.3.

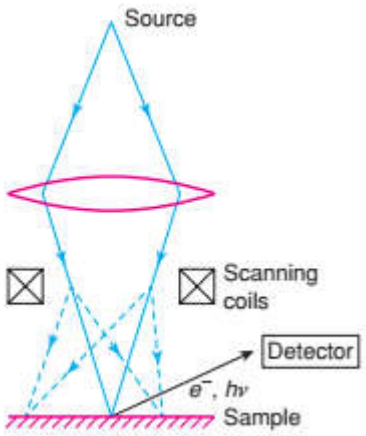

Figure 3.3: Principle of scanning electron microscope (SEM) [West (2014)]

The prepared pellets in our work were thoroughly polished with emery paper grade 0 to 4 .The fine polishing was done on blazer cloth using diamond paste (1µm). Then the pellets were thermally etched at a temperature 100^0C less than the sintering temperature for about 15 minutes to delineate the morphology. After etching, the samples were prepared for the 'conducting' mode SEM by sputtering silver-palladium or gold films for about 50 seconds onto the etched surface to prevent charge build up. The samples were then examined using the INSPECT S50 Scanning Electron Microscope. A systematic comparative study of the microstructure helps in identifying the morphology of the phase(s) present in the samples.

3.2.3 Electrical Characterization (MHz Range)

Complex impedance measurements were carried out by using Novocontrol Alpha-A Frequency Analyzer . The basic principle of measurement is as depicted in the sketch below in Figure 3.4 [Novocontrol technologies (2016)]. A voltage sinusoidal wave $V(t) = V_0 \cos \omega t$ of desired frequency ω and peak value V_0 is generated and fed to the sample sandwitched between two conducting plates and sample current I(t) is measured. From this, the amplitude I_0 and phase angle φ of the current harmonic base

wave component is obtained. For this Fourier transformation of I(t) over n periods is calculated to get

$$I^*(\omega) = I' + jI'' = \frac{2}{nT}\int_0^{nT} I(t)\exp(i\omega t)\,dt \quad \text{... (3.1)}$$

$$I_0 = \sqrt{I'^2 + I''^2} \quad ; \tan(\varphi) = \frac{I''}{I'} \quad \text{... (3.2)}$$

The value of impedance is then given by

$$Z^*(\omega) = Z' + jZ'' = \frac{V_0}{I^*(\omega)} \quad \text{... (3.3)}$$

Permittivity ε*(ω) and conductivity σ*(ω) are obtained by using

$$\varepsilon^*(\omega) = \varepsilon' - j\varepsilon'' = \frac{-j}{\omega Z^*(\omega)}\frac{1}{C_0} \quad \text{... (3.4)}$$

where C_0 is the empty cell capacitance and $j=\sqrt{(-1)}$. C_0 is calculated by measuring the area A of one of the parallel faces of the pellets and thickness d and using the relation

$$C_0 = \varepsilon_0 \frac{A}{d} \quad \text{... (3.5)}$$

where $\varepsilon_0 = 8.85 \times 10^{-12}$ Farad /meter.

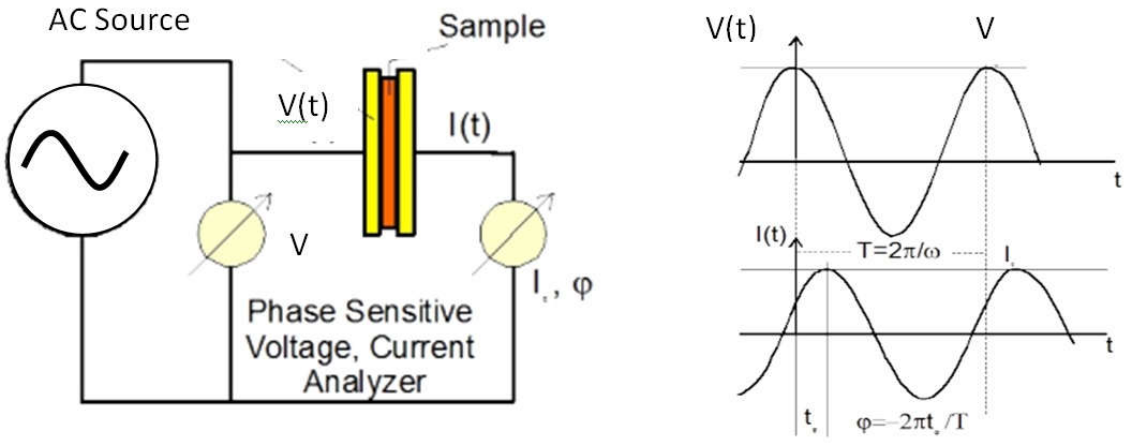

Figure 3.4: Schematic diagram of complex impedance measurement [Novocontrol Technologies (2016)].

Conductivity is obtained by using

$$\sigma^* = \sigma' - j\sigma'' = \frac{1}{Z^*(\omega)}\frac{d}{A} \quad \text{... (3.6)}$$

The electrical characterization namely measurement of the dielectric constant and dielectric loss are focused upon in this work. Overall dielectric and electrical properties of polycrystalline electronic ceramics have contributions from (i) bulk or grains (ii) grain boundaries and (iii) electrode specimen interface or electrode polarization. The complex permittivity and loss tangent are given as follows

$$\varepsilon^* = \varepsilon^{/} - i\varepsilon^{//} \qquad \tan\delta = \frac{\varepsilon^{//}}{\varepsilon^{/}} \quad \text{... (3.7)}$$

The pellets were properly polished with emery papers 0 to 4. They were then electroded using low temperature silver paste and heat treated for 15 minutes at a temperature of 200 ^{0}C in an electric oven. Dielectric measurements (the value of real and imaginary parts of permittivity) of the samples were carried out on these electroded pellets using two probe method in the frequency range 1 Hz to 1 MHz and at an interval of 25 °C in the range 20 – 250 °C in air using a Novovontrol Alpha-A High Performance Frequency Analyzer. Dielectric measurements were measured in a locally fabricated cell. The sample was placed on a plate welded to a stainless steel rod. Another spring-loaded electrode fixed in a stainless steel plate insulated by small circular cylinder pressed the sample from the top. The bottom plate and top rod served the purpose of two electrodes. These electrodes were connected to a Novocontrol Alpha- A High Performance Frequency Analyzer using shielded cables. The entire cell assembly was put in a stainless steel jacket for purpose of impedance measurements in the temperature range 23 – 250 °C. This whole assembly was slowly inserted into the

vertical furnace for heating. Values of Z′ and Z″ measured in this way were further used in impedance spectroscopy work also.

3.2.4 P-E Hysteresis Loop Measurement

Ferroelectric hysteresis loop measurements are carried out by using arrangements based on Sawyer and Tower (1930) circuit which is schematically shown in Figure 3.5 [Stewart et al (2014); Jaffe et al (1971)].

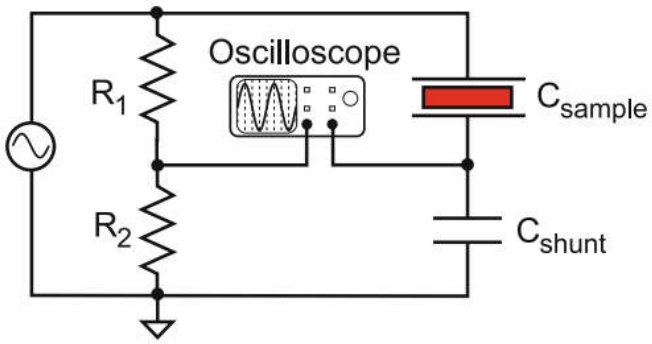

Figure 3.5: Schematic diagram of a Sawyer-Tower circuit for P-E loop measurement [Stewart et al. (2014)].

The potential devider having resistors R_1 and R_2 is used to attenuate the voltage applied to the sample. The capacitor C_{shunt} is in series with the sample so that charge flowing through them is the same. The high voltage plate of the shunt capacitor is connected to the Y-plates of oscilloscope and voltage applied to the sample is connected to the X-plates. The CRO measures the voltage V across shunt capacitor. If the capacitor C_{shunt} is of high quality and low leakage, the measured voltage can be used to give the charge (= C_{shunt} V) on the sample .The shunt capacitor is usually chosen to have a capacitance much larger than that of the sample.

Polarization hysteresis loop measurements for our samples were carried out by using AixACCT systems TF Analyzer 2000E, Germany, [aixACCT Systems (2018)]. The polarization is measured as the time integral of the current flowing during the

application of triangular voltage pulses, as done in Sawyer -Tower circuit, except that the current is integrated numerically by a computer instead of by a capacitor.

3.2.5 Electrical Characterization (GHz Range)

Measurement of dielectric permittivity ($\varepsilon^* = \varepsilon' - j\,\varepsilon''$) and magnetic permeability of materials can be carried out by various methods that can be put under two categories (i) resonant methods and (ii) non- resonant methods [Chen et al.(2004); Sebastian (2008); Sebastian et al. (2017)]. In resonant methods use is made of resonance frequency of the dielectric sample itself (called the resonator method) or of the shift produced in the resonance frequency of a structure when a sample is inserted in it (known as resonant perturbation method). In non-resonant methods use is made of reflection and transmission of a microwave signal directed towards the sample. The resonant methods are more accurate but give the values of parameters at fixed frequencies whereas in non-resonant methods frequency can be swept and parameters are obtained as a function of frequency. One of the popular resonant methods is the Hakki- Coleman resonator [Hakki et al. (1960); Chen et al. (2004)]. It was further developed by Courtney and therefore is also called Courtney resonator [Courtney (1970)]. The sample is placed between two large conducting grounded plates and two probes are placed near the sample to excite and measure electromagnetic fields. The sample acts as dieletric resonator. Sample of a given size resonates at a certain frequency. So several sample of various dimensions are needed to cover a desired frequency range.

A closed cylindrical or rectangular cavity is used in the so called cavity – perturbation methods. The resonance frequency of a cavity of given dimensions is known. The cavity is excited in a given mode. The sample of a shape similar to the

cavity is placed in the cavity and resonance frequency is determined. From the shift in frequency, the material parameters of the sample are calculated. The sample is placed at the location of maximum electric field inside the cavity to obtain the value of permittivity and at maximum magnetic field to get the value of permeability [Chen et al. (2004)].

The non-resonant methods, such as the so popular Nicholson-Ross-Wier method, utilize the change in behaviour of microwaves propagating through the air-sample-air system for obtaining the values of permittivity and permeability of the sample. A medium has a characteristic impedance Z_0 governed by its dielectric permittivity and permeability. An electromagnetic wave propagating through a medium has certain velocity and wave impedance. When a propagating electromagnetic wave passes from one medium to another, its wave impedance and velocity change. As a result reflection and transmission take place at the boundary separating the two media. For example, for microwave propagating in air and passing through a dielectric sample would suffer reflection and transmission at the air - sample boundary when it enters the sample and again at sample-air boundary while coming out of it. Measurement of reflected and transmitted parts are used to obtain values of permittivity and permeability of the sample. Thus, non-resonant methods need means to carry a microwave towards the sample, and means to measure the reflected part and to measure the transmitted part. All transmission lines, such as coaxial line, planar transmission line, hollow metallic wave guide, dielectric wave guide and free space, can be used to direct a microwave towards the sample.

The values of dielectric permittivity and permeability at microwaves were measured in our work by using Keysight E5071 Network Analyzer [Keysight (2016)].

The working is based on the Nicholos-Ross-Wier method which is a reflection/transmission method [Keysight (2016); Luukkonen et al. (2011); Nicolson et al. (1970); Weir (1974); Tripathi et al. (2015); Baker-Jarvis et al. (1993); Baker-Jarvis (1990)]. The sample holder consists of a rectangular waveguide with two coaxial ports. The sample having cross-section just fitting with the inner cross-section of the wave guide is placed inside such that the thickness of the pellet is along the axis of the wave guide. The two ports are used to measure scattering parameters (S-parameters) which are related to the power reflected from the sample and transmitted through it. When a wave initially travelling in air (permittivity ε_0, permeability μ_0, characteristic impedance Z_0) enters the sample (permittivity ε_r, permeability μ_r, characteristic impedance Z) of thickness 'd', it suffers partial reflection and transmission at the air-sample interface. The transmitted part traverses a distance 'd' in the sample and, while going out of the sample, gets partly reflected again at the sample – air interface. The transmitted wave then further propagates in air. The relative permittivity ε_r^* and relative permeability μ_r^* are computed from the measurement of the reflected signal (S_{11}) and transmitted signal (S_{21}) using the expressions given below

$$\mu_r^* = \frac{1+\Gamma}{\Lambda(1-\Gamma)\sqrt{\left(\left(\frac{1}{\lambda_0^2}\right)-\left(\frac{1}{\lambda_c^2}\right)\right)}} \qquad ...(3.8)$$

$$\varepsilon_r^* = \frac{\left(\left(\frac{1}{\Lambda^2}\right)-\left(\frac{1}{\lambda_c^2}\right)\right)\lambda^2}{\mu_r^{*2}} \qquad ...(3.9)$$

where λ_0 is the free space wavelength , λ_c is cutoff wavelength for fundamental TE_{10} mode in the waveguide and Λ is given as

$$\frac{1}{\Lambda^2} = -\left[\frac{1}{2\pi d}\ln\left(\frac{1}{T}\right)\right]^2 \qquad ...(3.10)$$

Here, d is the thickness of the sample. Γ and T are reflection and transmission coefficients respectively.

The reflection coefficient Γ is given as

$$\Gamma = K \pm \sqrt{K^2 - 1} \qquad ...(3.11)$$

where K is given by

$$K = \frac{[S_{11}^2 - S_{21}^2] + 1}{2\,S_{11}} \qquad ...(3.12)$$

The value of T is given by

$$T = \frac{S_{11} + S_{21} - \Gamma}{1 - (S_{11} + S_{21})\Gamma} \qquad ...(3.13)$$

Basics of the derivations of above equations are given in Appendix A. The scattering parameters S_{11}, S_{12} etc are defined in the following way. Consider a two- port network (one input port and one output port implying two input terminals and two output terminals). Let a_1 be the incidence parameter (which is proportional to the incidence voltage) at the input side. Similarly , let a_2 be incidence parameter (which is proportional to the incidence voltage) at the output side. Then the reflected parameters b_1 and b_2 at the input and output side respectively can be expressed as

$$b_1 = S_{11}a_1 + S_{12}a_2 \qquad ...(3.14)$$

$$b_2 = S_{21}a_1 + S_{22}a_2 \qquad ...(3.15)$$

The scattering parameters (coefficients) are given as

$$S_{11} = \frac{b_1}{a_1}\Big|_{a_2=0} \qquad \text{Input reflection coefficient} \qquad ...(3.16)$$

$$S_{12} = \frac{b_1}{a_2}\Big|_{a_1=0} \qquad \text{Reverse transmission coefficient} \qquad ...(3.17)$$

$$S_{21} = \frac{b_2}{a_1}\Big|_{a_2=0} \qquad \text{Forward transmission coefficient} \qquad ...(3.18)$$

$$S_{22} = \frac{b_2}{a_2}\Big|_{a_1=0} \qquad \text{Output reflection coefficient} \qquad ...(3.19)$$

For a reciprocal system $S_{12} = S_{21}$ [Baker-Jarvis 1990].